Injection of Supercritical Carbon Dioxide into Granitic Rock and its Acoustic Emission Monitoring

AUTHOR(S):

Ishida, Tsuyoshi; Desaki, Shuich; Yamashita, Hiroto; Inui, Shuhei; Naoi, Makoto; Fujii, Hirokazu; Katayama, Tatsuo

CITATION:

Ishida, Tsuyoshi ...[et al]. Injection of Supercritical Carbon Dioxide into Granitic Rock and its Acoustic Emission Monitoring. Procedia Engineering 2017, 191: 476-482

ISSUE DATE:

2017

URL:

http://hdl.handle.net/2433/234999

Available online at www.sciencedirect.com

ScienceDirect

Procedia Engineering 191 (2017) 476 – 482

Procedia Engineering

www.elsevier.com/locate/procedia

Symposium of the International Society for Rock Mechanics

Injection of Supercritical Carbon Dioxide into Granitic Rock and its Acoustic Emission Monitoring

Tsuyoshi Ishida[a,]*, Shuich Desaki[a], Hiroto Yamashita[a], Shuhei Inui[a], Makoto Naoi[a], Hirokazu Fujii[b], Tatsuo Katayama[c]

[a]*Kyoto University, C-Cluster, Katsura Campus of Kyoto University Nishikyo-ku, Kyoto 615-8540, Japan*
[b]*LAZOC Inc., 1-5-3, Nishikameari, Katsushika-ku, Tokyo, 124-0002, Japan*
[c]*KANSO Co., Ltd.,1-3-5, Azuchi-cho, Chuo-ku, Osaka, 541-0052, Japan*

Abstract

We injected carbon dioxide (CO_2) into a hole drilled around 8 m long in a granitic hot rock from the floor of the tunnel. We drilled four AE (acoustic emission) monitoring holes parallel 1 m far away from the injection hole and monitored AE events induced with hydraulic fracturing (HF). When the breakdown (BD) pressure was recorded, the pressure and the temperature satisfied the supercritical condition of CO_2. The AE source distribution showed that two vertical cracks were initiated from the injection hole with BD. After 75 seconds from the occurrence of BD with no pressure increase, the AE sources started to distribute along the direction almost normal to that of the initial crack from the position around 0.7 m far away from the injection hole. It is most likely that the cracks initiated in intact rock with BD by HF and one of them bended and extended along pre-existing crack. These results suggest that CO_2 migrates easily and enhances AE occurrence in a pre-existing joint.

Peer-review under responsibility of the organizing committee of EUROCK 2017

Keywords: Carbon dioxide, Hydraulic fracturing; Acoustic emission; Field experiment; Pre-existing joint; Breakdown

1. Introduction

The carbon capture and storage (CCS) in underground is a promising and feasible method for mitigating the greenhouse effect by decreasing the amount of CO_2 emissions. If we can utilize CO_2 for energy production

* Corresponding author. Tel.: +81-75-383-3209.
E-mail address: ishida.tsuyoshi.2a@kyoto-u.ac.jp

Peer-review under responsibility of the organizing committee of EUROCK 2017
doi:10.1016/j.proeng.2017.05.206

and compensate for the cost of CCS, which is called carbon capture, utilization and storage (CCUS), CCS will be much more eagerly developed and adopted. For example of CCUS, Xie et al. [1] shows enhance the recovery of oil (CO_2-EOR), coalbed methane (CO_2-ECBM), geothermal systems (CO_2-EGS), natural gas (CO_2-EGR), shale gas (CO_2-ESG) and others.

For EGS, EOR, ESG and ECBM, CO_2 is usually injected into rocks at a depth of more than 1000 m and sometimes more than 3000 m, and the temperature and pressure at these depths make CO_2 supercritical state. The viscosity of supercritical CO_2 (SC-CO_2) is one or two order of magnitude smaller than that of normal liquid water. To examine effect of fracturing fluid viscosity on a crack features induced by hydraulic fracturing (HF), Ishida et al. [2, 3] made HF experiments using SC-CO_2, liquid CO_2 (L-CO_2), water and viscous oil in 170×170×170 mm cubic granite blocks with a center hole of 20 mm diameter. They found in the laboratory experiments that fracturing with low-viscosity fluid such as SC-CO_2 tends to induce three-dimensionally sinuous cracks with many secondary branches, which seem to be desirable pathways for EGS, ESG and ECBM. However, the effect of fracturing fluid viscosity on HF in real rock mass including pre-existing cracks has not been still clarified. Thus, we made small field HF experiment using CO_2 in a hot rock mass under a tunnel floor which satisfies the temperature to form SC-CO_2, and monitored acoustic emission (AE) induced by HF to clarify crack extension.

2. Site and experimental setup

2.1. Site and method of CO_2 injection

The site was a small tunnel in a depth of around 50 m from the surface of the mountain area of Kurobe, central Japan, which has hot granitic rock mass formed from the late Miocene to the Pleiocene. As shown in Fig. 1 and 2, an HF hole was drilled downward around an eight meter from the tunnel floor and four AE monitoring holes were drilled parallel 1 m far away from the HF hole. Since the water level was around 1 m below the tunnel floor, the all experiments were made in a rock mass saturated with water. To inject CO_2, we drilled a 36 mm small diameter pilot hole at the bottom of the 86 mm large diameter HF hole. To drill the pilot hole at the center of the bottom of the large diameter hole, before drilling the pilot hole, we making the bottom of the large diameter hole in conical shape using a specially designed diamond bit as shown in Fig. 3(a). To inject CO_2, we sealed the upper section of the pilot hole with an O-ring equipped on the packer unit and poured cement paste above the O-ring, as shown in Fig. 3(b). The sealed section for injection was 0.16 m long from 7.24 to 7.40 m depth from the floor of the tunnel. After performing HF using CO_2 in the section, we over-cored the section with the 86 mm diameter drilling bit to inspect cracks induced by the HF. By repeating this procedure, we injected CO_2 four times and water three times. Among the seven trials, we report only one experiment that we could make HF with CO2 successfully without leaking.

Fig. 4 shows the injection system used for the experiments. We used two syringe pumps to inject CO_2 continuously without stop. We fed CO_2 from a bomb to two syringe pump cylinders, which had a capacity of 500 mL for each. To fill the cylinders as full as possible, we cooled the CO_2 in the cylinders to keep it in the liquid state by circulating coolant using a cooling unit. The phase diagram in Fig. 5 shows that CO_2 becomes supercritical under the temperature higher than 31°C and the pressure greater than 7.38 MPa. After discharging L-CO_2 from the cylinder of the syringe pump at a constant flow rate of 50 mL/min, we heated it the temperature of around 50°C with a heater unit and injected it into the sealed section in the rock having the temperature of 35°C and saturated with water.

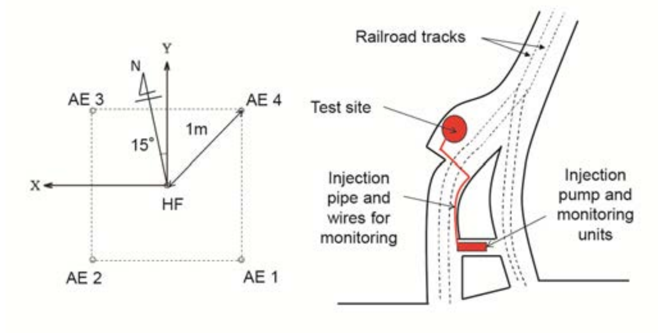

Fig. 1. Outline of test site (right) and borehole layout in the test site (left).

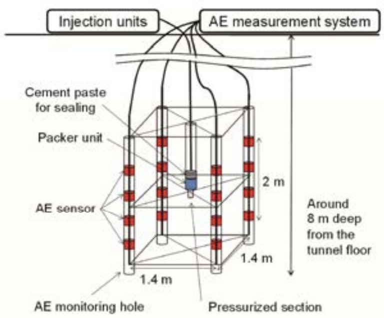

Fig. 2. Arrangement of the AE sensors to enclose the pressurized section.

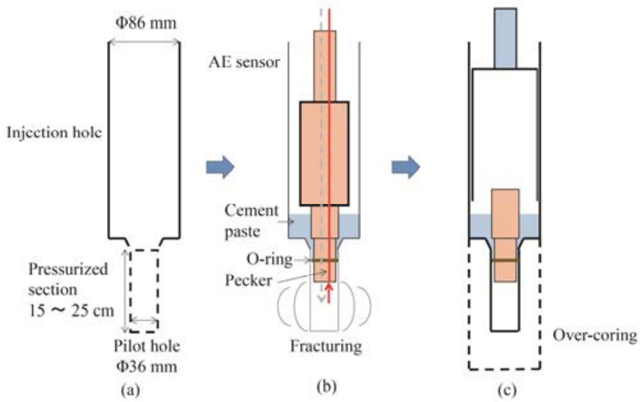

Fig. 3. Procedure of drilling. (a)Drilling of a pilot hole; (b)Fracturing with CO_2 injection into the pilot hole sealed by a pecker with O ring and cement paste; (c)Over coring to inspect cracks induced by the fracturing.

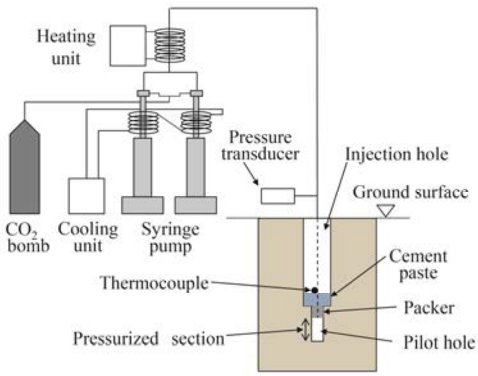

Fig. 4. Injection system for SC-CO_2.

2.2. Methods for monitoring AE, pressure, and temperature

For the AE monitoring, we used a waterproof sensor with a resonance frequency of 70 kHz (Fuji Ceramics Corporation, AE703SW) set in the four holes (see Fig. 2). We fixed the sensor onto an aluminum rod with a very small hydraulic jack and a pre-amplifier, inserting a thick rubber sheet between the sensor and the rod to shut out vibration transmitted through the rod. After facing the sensitive direction of the sensors toward to the injection hole, by applying and keeping the oil pressure of 1.5 MPa to the jack set behind each of the sensor, we pressurized the sensor onto a wall of the AE monitoring hole drilled 1 m far away from the injection hole. In the respective AE monitoring hole, we set the four sensors in a 2 m long span with intervals of 0.6 or 0.7 m so as to center the span at the depth of the pressurizing section of the injection hole (see Fig. 2).

The recording of an AE event was triggered when one of the signals from the 16 AE sensors in total set in the four holes exceeded 1 V. After AE signals detected at the sensors were amplified by 30 dB in a pre-amplifier and 40 dB in a signal conditioner, they are processed with a band-pass filter between 20 and 200 kHz, and recorded on a hard disk through an analog-to-digital (A/D) converter (PXI-5105, National Instruments Corp.). The A/D converter has 16 separate channels, and the processed AE signal for each event and for each sensor were digitized into 2048 samples with 1 μs sampling time. We set the dead time to stop recording for 10 ms just after recording an event for 204.8 μs, to prevent the hard disk from recording too much noise caused by "ringing", which is the vibration following a large AE event.

Every 0.1 s, we measured the injected fluid pressure with a transducer (PW-50MPA, Tokyo Sokki Kenkyujo Co., Ltd.) set on the injection pipe just outside of the HF hole, and measured the temperature change with a T-type thermocouple glued to the injection pipe just above the cement paste to seal the pressurize section in the hole.

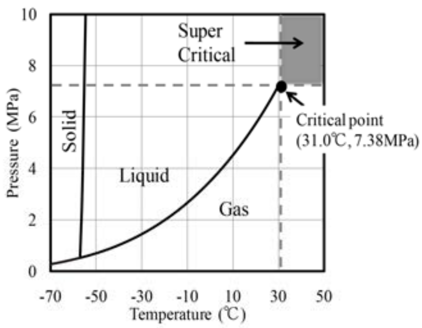

Fig. 5. Phase diagram of CO_2.

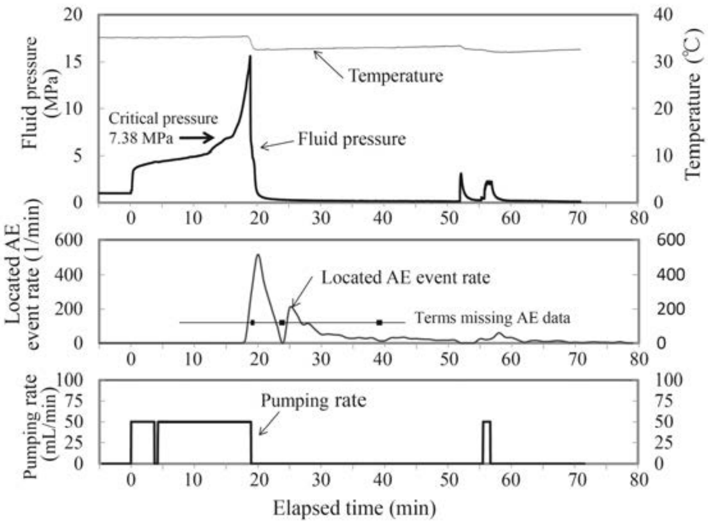

Fig. 6. Changes in injected fluid pressure, temperature, located AE event rate and flow rate. Thick line segments on the fine line in the middle figure indicate terms missing AE data.

3. Results and discussion

3.1. Changes in fluid pressure, temperature, located AE event and flow rate

Fig. 6 shows the changes in injected fluid pressure, temperature, located AE event rate and flow rate. When we opened the valve of the injection system, the bomb pressure around 1 MPa applied to the pressurized section, since we fed CO_2 from the bomb. We injected CO_2 in the constant flow rate of 50 mL/min, with the sudden stop from 3 min 42 s to 4 min 12 s after starting the injection due to a trouble at switching the two syringe pumps. The injected pressure increased with the elapsed time, HF was induced at the breakdown (BD) pressure of 15.62 MPa, which is defined as the peak pressure just before large sudden pressure drop at 18 min 55 s. Just after the BD, the injection was stopped. A few minutes later after the BD, we found that bubbles of CO_2 are gushing out from the AE monitoring holes No. 1 and No. 3. When we opened a valve at 55 min 34 s, the pressure increased to 3.07 MPa due to the pressure remained in the injection system. After the pressure was released, to reopen the induced crack and monitor associate seismicity, we reinjected CO_2 again from 55 min 35 s to 56 min 40 s in the flow rate of 50 mL/min. With the reinjection, CO_2 gushed out again from the AE monitoring holes No. 1 and No. 3, and the injected pressure did not increase more than 2.27 MPa.

In Fig. 6, we showed the temperature measured with the thermocouple glued to the injection pipe just above the cement paste to seal the pressurize section. Referring to the phase diagram of CO_2 shown in Fig. 5, we can infer that CO_2 was in gas state when the test began and started to change into supercritical state when the pressure get closer to 7.38 MPa. This change could be inferred from the change in the increase rate of the fluid pressure under the constant flow rate as shown with the arrow in Fig. 6. This change was most likely caused by the decrease of the fluid compressibility due to the change from the gas to the supercritical state of CO_2. The pressure decreased sharply just after BD at 15.62 MPa. Due to the pressure decrease caused by leakage through induced cracks, CO_2 become gas again from supercritical state. The temperature also decreased to 32.6 °C just after BD. The temperature decrease was probably caused by adiabatic expansion of CO_2.

There were three terms missing AE data as shown with the thick solid line segments in the middle of Fig. 6. The first missing term from 18 min to 19 min 22 s was due to a trouble in AE data acquisition by too many AE events induced. The second and third terms, from 23 min 34 s to 25 min 8 s and 39 min 27 s to 40 min 40 s, respectively, were due to replacing a file filled with AE data in the monitoring unit. The decreases in the located AE event rate in the second and third terms were caused by the missing data.

3.2. AE Source locations

As source location method, we adopted the iterative method with the least square principle, using P wave arrival time. An average P wave velocity measured between the AE sensors in the respective monitoring holes and an emitter set in the injection hole was 5.4 km/s with the standard deviation of 0.4 km/s. Since the scattering in the P wave velocity due to the inhomogeneity is larger than the anisotropy, we used the average velocity to locate AE sources without considering the anisotropy. The accuracy of the source location is expected within 50 mm by satisfying the following criteria [4]: (i) six or more P wave arrival times could be read; (ii)

AE sensors in which the P wave arrival times were read distributed more than three monitoring holes so that the sensors surround a source three dimensionally; (iii) the standard deviation and the maximum of residuals of arrival times were within 10 and 20 μs respectively. Satisfying these conditions, we located the sources of 1463 AE events during the CO_2 injection, excepting those in the three data missing terms.

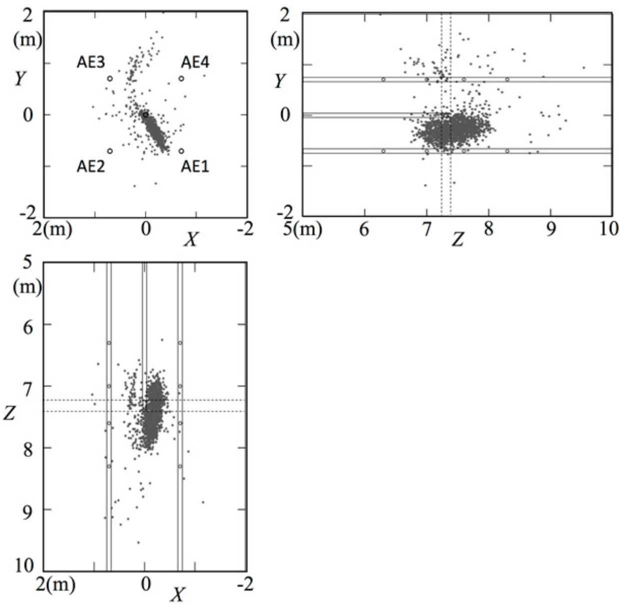

Fig. 7. Locations of AE sources projected onto the horizontal plane, *XY*, and the two vertical planes, *YZ*, and *ZX*.

Fig. 7 shows the locations of AE sources observed during the fluid injections projected onto the horizontal plane, *XY*, and the two vertical planes, *YZ*, and *ZX*. On the two vertical planes, we can see that they distributes on a little bit larger area in lower direction rather than upper from the pressurized section indicated between the two dotted lines. Fig. 8 shows AE source distributions on the horizontal *XY* plane, for the period from 0 to 75 s after BD (from 18 min 55s to 20 min 10 s in the elapsed time) in comparison with those from 0 to 1500 s (43 min 55 s).

The figure indicates that AE sources distributed along A direction from the HF hole to AE1 and AE3 hole for 75 s from BD. After that, they started to distribute in B-direction almost normal to A direction from the portion close to AE3 hole. Since the large BD pressure, 15.62 MPa, was recorded, we can infer that new cracks were induced at BD and it extended for 75 s along A direction. The direction of the crack extension corresponds to the observation that the injected CO_2 gushed out from the holes AE1 and AE3. In contrast, in spite of no pressure increase for the term after BD to 1500 s as shown on Figure 6, AE sources distributed along B direction from the position around 0.7 m distant from the HF hole. Also from the fact that the distributed direction was normal to A direction, we can infer that the AE events were induced with intrusion of CO_2 into a pre-existing joint.

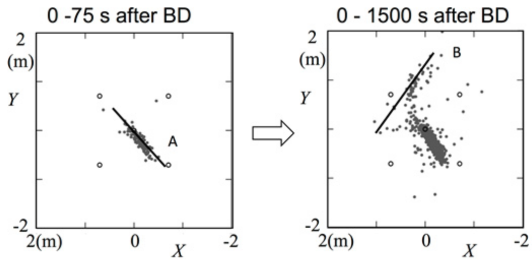

Fig. 8. Locations of AE sources projected onto the horizontal plane, *XY*, for the period from 0 to 75 s after BD (left-hand side) in comparison with those from 0 to 1500 s (right-hand side).

4. Conclusion

We made HF using CO_2 in the hole in a granitic hot rock at the depth of 7.24 to 7.40 m below the tunnel floor. We monitored AE with 16 sensors in the four holes drilled parallel 1 m far away from the HF hole. When BD was recorded, the pressure and the temperature satisfied the condition to form SC-CO_2. The AE source distribution showed that two vertical crack planes initiated from the injection hole with BD. After 75 s from the occurrence of BD, in spite of no pressure increase, the AE sources started to distribute along the direction almost normal to that of the initial crack from the position around 0.7 m far from the injection hole. It is most likely that the cracks initiated in intact rock with BD by HF and it bended and extended along pre-existing crack. These results suggest that CO_2 migrates easily and enhances AE occurrence in a pre-existing joint. We are now making further analysis of the AE data, and have a plan to make more field experiments.

Acknowledgements

This work was financially supported by the Japan Society for the Promotion of Science Grants-in-Aid for Scientific Research (A), Grant Numbers 25249131.

References

[1] H. Xie, X. Li, Z. Fang, Y. Wang, Q. Li, L. Shi, B. Bai, N. Wei, Z. Hou, Carbon geological utilization and storage in China: current status and perspectives, Acta Geotechnica 9 (2014) 7–27.

[2] T. Ishida, K. Aoyagi, T. Niwa, Y. Chen, S. Murata, Q. Chen, Y. Nakayama, Acoustic emission monitoring of hydraulic fracturing laboratory experiment with supercritical and liquid CO2, Gephys. Res. Lett. 39 (2012) L16309.

[3] T. Ishida, Y. Chen, Z. Bennour, H. Yamashita, S. Inui, Y. Nagaya, M. Naoi, Q. Chen, Y. Nakayama, Y. Nagano, Features of CO_2 fracturing deduced from acoustic emission and microscopy in laboratory experiments, J. Geophys. Res. Solid Earth, 121 (2016) doi:10.1002/2016JB013365.

[4] T. Ishida, S. Sasaki, Numerical simulation to examine accuracy of AE source location and its applications to in-situ rock monitoring, J. Acoust. Emission 29 (2011) 260–272.